




Article

Detection and Classification of Recessive Weakness in Superbuck Converter Based on WPD-PCA and Probabilistic Neural Network

Chenhao Wu ¹, Jiguang Yue ^{1,*} and Feng Lyu ²

¹ College of Electronic and Information Engineering, Tongji University, No. 4800, Cao'an Highway, Shanghai 201804, China; 1152448@tongji.edu.cn (C.W.); yuejiguang@tongji.edu.cn (J.Y.)

² School of Ocean and Earth Science, Tongji University, No.1239, Siping Road, Shanghai 20092, China; lf@tongji.edu.cn

* Correspondence: 2015wangli@tongji.edu.cn; Tel.: +86-021-6598-9241

Received: 1 February 2019; Accepted: 28 February 2019; Published: 5 March 2019



Abstract: This paper proposes a detection and classification method of recessive weakness in Superbuck converter through wavelet packet decomposition (WPD) and principal component analysis (PCA) combined with probabilistic neural network (PNN). The Superbuck converter presents excellent performance in many applications and is also faced with today's demands, such as higher reliability and steadier operation. In this paper, the detection and classification issue to recessive weakness is settled. Firstly, the performance of recessive weakness both in the time and frequency domain are demonstrated to clearly show the actual deterioration of the circuit system. The WPD and Parseval's theorem are utilized in this paper to feature the extraction of recessive weakness. The energy discrepancy of the fault signals at different wavelet decomposition levels are then chosen as the feature vectors. PCA is also employed to the dimensionality reduction of feature vectors. Then, a probabilistic neural network is applied to automatically detect and classify the recessive weakness from different components on the basis of the extracted features. Finally, the classification accuracy of the proposed classification algorithm is verified and tested with experiments, which present satisfying classification accuracy.

Keywords: fault detection; superbuck converter; wavelet packet decomposition (WPD); principal component analysis (PCA); probabilistic neural network (PNN)

1. Introduction

As the vital energy source of the power system in spacecraft, a switching power converter plays a crucial role in the success of a space mission. In recent years, the Superbuck converter has gradually become the typical topological structure of the space power supply, because of its low EMI (Electro-Magnetic Interference) noise and capacitor current [1,2]. More than 90 percent of spacecrafts domestically and overseas adopt such power systems for energy conversion. A fault in the circuit is unexpected and unavoidable, which is caused by many reasons, so it is of great significance to fault detection and diagnosis [3]. The recessive weakness of component parameters in a circuit is even more complicated to identify and detect, presenting unsteady inner system performance without a dominant output character difference from the normal operating situation.

There exist already some established fault detection and classification methods for different kinds of power converters. The discrete wavelet transform has been applied in the detection of current waveform in a direct current system [4]. The shortcoming of this method is that all of the wavelet decomposition coefficients are chosen as the feature vector, which complicate the training process and increase the computing time. A support vector machine (SVM) is used to diagnosis the soft

fault in an analog circuit. But the final classification accuracy is far from satisfactory [5]. The fuzzy math and the direction vector of the voltage increment are combined together in the diagnosis of the analog circuit fault. However, the accuracy of this method is easily influenced by the disturbances and noises [6]. A method for online inverter fault diagnosis of a buck converter is designed to deal with the open circuit and short circuit fault rapidly and effectively. The soft faults are not considered, because they are more difficult and significant to be settled down [7]. A model-based fault detection and identification method has been proposed for arbitrary faults in components within a broad class of switching power converters. However, the experimental design of the kinds of fault cannot cover all the possible conditions [8].

In this paper, a new method combined with wavelet packet decomposition and a probabilistic neural network is designed for fault detection and the classification of recessive weakness in a Superbuck converter. The characteristics and seriousness of recessive weakness are obviously demonstrated through simulation in both time domain and frequency domain. Furthermore, the wavelet packet decomposition provides a more precise analysis method for signals with the continuous decomposition of both low frequency and high frequency data [9]. Moreover, the proposed approach uses the advantage of PCA to reduce the dimension of feature vectors to achieve higher efficiency [10]. In contrast to a BP (Back Propagation) network, the probabilistic neural network presents a greatly improved training speed and steady convergence to the bayesian optimization solution [11,12].

The fault detection schemes for the recessive weakness of a Superbuck converter are still in the early stages of development as a result of the growing requirement of lighter weight and higher reliability. The presented method shows a high classification accuracy to recessive weakness throughout a series of experiments.

2. Recessive Weakness in Superbuck

2.1. Superbuck Converter

A Superbuck converter, known as a double inductance buck circuit, can obtain continuous current, small voltage ripple and input output voltages of the same polarity [13]. It is derived from the buck converter and combines with the input inductor-capacitor filter to achieve the same output gain as the buck circuit. Due to the continuity of its input and output currents, a Superbuck converter is generally suited to a power factor correction (PFC) and the connection between photovoltaic panels and the battery. Furthermore, coupled inductors can realize the requirement of lighter weight and minor volume, so the Superbuck converter is widely applied as a power function unit of a satellite [14].

As a current source type buck converter, the basic principle is through the open and closed status of the switch Q to realize the control of the output voltage. The main topology of the Superbuck converter is shown in Figure 1, where V_{in} , V_o , represent the input and output voltage; double inductance are L_1 , L_2 ; double capacitance are C_1 , C_2 . L_1 is the input inductance and L_2 the energy storage inductance, which promise that both the input and output current maintain consistency [15]. In the design of a Superbuck converter, these two inductances L_1 & L_2 , are not magnetically coupled as graphically demonstrated in Figure 1. The relationship between output and input can be expressed as $\frac{V_{out}}{V_{in}} = D$, D presents the duty ratio of the switch. The parameters of a Superbuck converter are listed in Table 1.

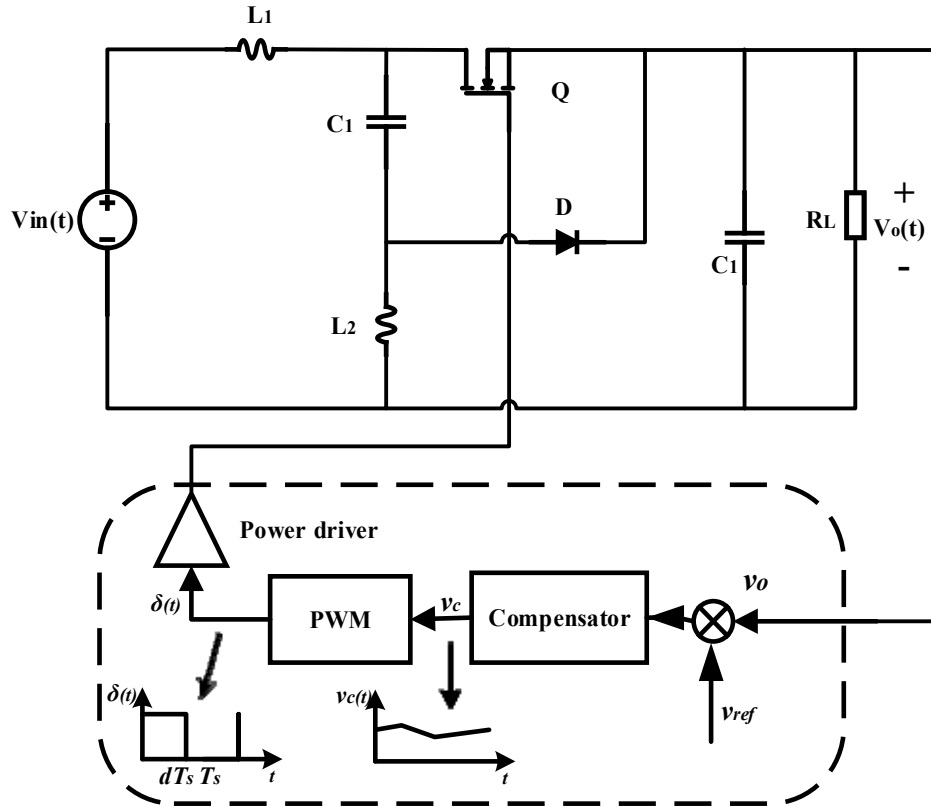
The Superbuck converter only adds one inductance and capacitance to achieve zero ripple input current and continuous output current. The structure of Superbuck converter is shown in Figure 1. and the feedback loop consist of compensator, pulse width modulation (PWM), and power drive.

Analyze the operating status of the Superbuck converter in CCM (Continuous Conduction Model) of one period as follows:

$T_0 \sim dT_s$: While the Switch Q is turned off, the diode D is on and the inductor obtains the continuous current through the diode D and load resistor R_L . The inductor L_1 charges the capacitor C_1 which causes the linear decline of inductor current. Since the end voltage of L_2 is positive, the inductor L_1 , the diode D and the load resistor R_L constitutes a circuit.

Table 1. The parameters of Superbuck converter.

Parameter	Value	Parameter	Value
$L_1/\mu\text{H}$	220	$V_{in}(t)/\text{V}$	42
$L_2/\mu\text{H}$	110	$V_o(t)/\text{V}$	12
$C_1/\mu\text{F}$	2.5	D	0.286
$C_2/\mu\text{F}$	10	R_L/Ω	12

**Figure 1.** Structure of the Superbuck converter.

$dT_s \sim T_1$: While the Switch Q is turned on, the diode D is off and the input current passes through the inductor L_1 directly to the load resistor R_L . The capacitor C_1 simultaneously depend on the inductor L_2 to spread energy to the load, the inductor L_2 , the capacitor C_1 , the switch Q and the load resistor R_L forms a circuit, thus both the current of inductor L_1 and L_2 achieve the linear ascent.

2.2. Recessive Weakness

Fault in the circuits refers to the deviation of at least one feature order parameter in a system, which is beyond the acceptable range. The consequence is that the performance of the system is outside the normal level and is not capable of the expected function. Analog circuit faults can be classified into a catastrophic fault and a performance degradation fault [16]. The catastrophic fault is the open fault and short fault in the circuit, namely the hard fault; the performance degradation fault is the drift out of the tolerance range of the normal value in the component parameter without failure of the whole component function, namely the soft fault.

When the power converter operates in the environment of extreme temperature and other complex application conditions, it may accelerate the parameter degradation of the components in the circuit. Take the space power Superbuck converter as an example, it has two capacitors, two inductors, one diode and one transistor. In total there are six key components to fulfil the circuit principle and meanwhile burden the circuit operation. If the soft fault of these components occurs without timely,

accurate and effective methods of detection, it may lead to inestimable loss and serious catastrophe to the entire system and mission.

In a Superbuck converter, if the filter capacitance C_2 is beyond the tolerance range, longer rising time and steady time will cause 50% over rated value. Similarly, the condition of 50% under rated value will lead to unexpected filtering effects and larger ripple waves. The loss of capacitance C_1 will cause the larger overshoot and longer steady time, which are the important dynamic indicators of the system. Moreover, the increase of C_1 will also cause unsteady voltage and a larger ripple wave. The change of L_1 and L_2 can result in unsteady output voltage and continuous oscillation, which seriously influence the system response character. Furthermore, the variation of C_1 , L_1 and L_2 will greatly transform the system transfer function (relationship between input and output). Without timely detection, recessive weakness will bring out the failure of the whole converter function. The damage occurs to both sides of the input and output units in the circuits.

Obviously, recessive weakness is a kind of soft fault, resulted from the synchronous variation of more than two components in a circuit, which is characterized by recessive change in an output curve and actually more deteriorated stability in system. Any hard fault of the parameter in the Superbuck converter can lead to a dominant change of the output character curve directly and alter the system operating situation. The recessive weakness of more than two parameters concurrently may lead to the wave mutation as a normal situation without apparent change because of the mutual effect of components. The output signal from the recessive weakness is quite analogous, for instance, in the steady state output voltage or the ripple output voltage. The whole Supberbuck system character, such as the Amplitude Margin (AM) Phase Margin (PM), virtually become weaker and unsteady. In consequence, the physical meaning and feature of “recessive” is prominent and outstanding.

If the recessive weakness of the critical component in the circuit occurs with normal output performance then the deteriorative system property may lead to the invalidation of the circuit, or even the failure of the whole function task. On account of the imperceptible and undetectable characteristics of the recessive weakness, it is of great importance to detect and classify the recessive weakness in a timely manner to guarantee and maintain the operation of the power supply system.

2.3. Time Domain Performance

Figure 2 shows the output curve within the same range (10%) of the single change of the inductance L_1 , L_2 and the recessive weakness of both inductance L_1 & L_2 (synchronously) in contrast to the normal situation [17]. The results from the simulation in the time domain show some visible differences of the dynamic performance, such as overshoot, rise time and response time, while because of the existence of the feedback loop of the circuit, the steady output is always adjusted and reaches the steady state. Therefore, the steady output voltage is nearly identical without obvious distinction. To the contrary, the ripple wave of the recessive weakness from L_1 , L_2 is more similar to the normal situation compared with the single change of L_1 and L_2 , which makes it even more difficult to distinguish the recessive weakness in the Superbuck converter.

Apparently, the output character caused by the recessive weakness of the two crucial components simultaneously is approximate to the normal output signal and this inner-system recessive weakness can be easily ignored, considering the output character alone. Since the time domain performance of recessive weakness shows hardly no distinguishable difference, the detection of recessive weakness in the frequency domain is considered.

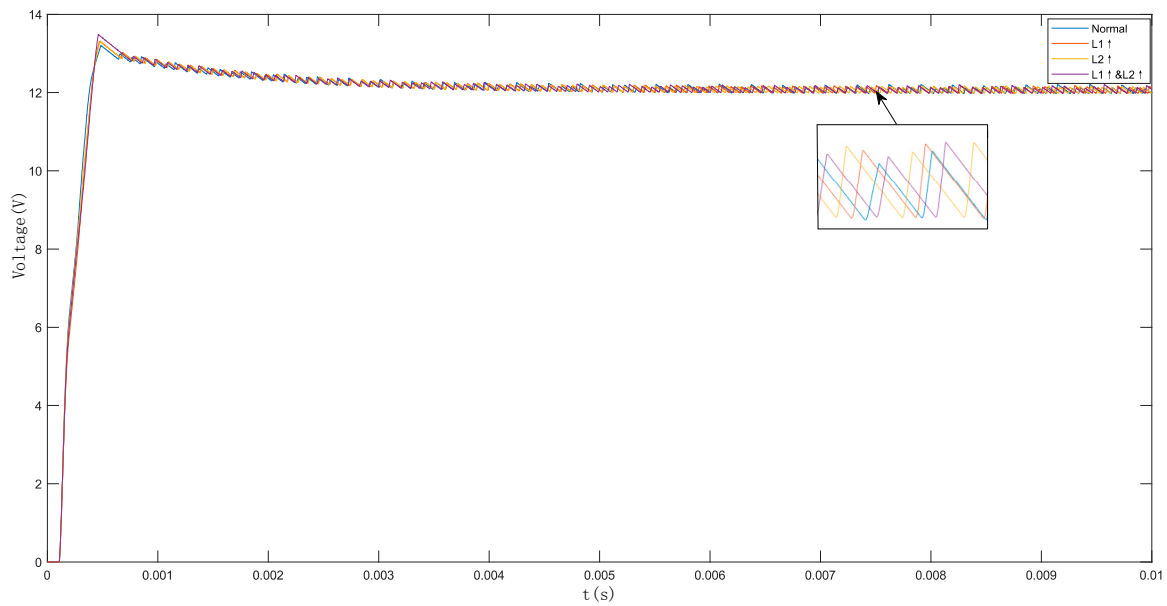


Figure 2. Output response of the Superbuck converter with recessive weakness.

2.4. Frequency Domain Performance

The system character aroused by recessive weakness can be also identified by transfer function $G_{vd}(s)$ in the frequency domain. Since the Superbuck converter has two capacitors and two inductors, its small signal model is a fourth-order system. The small signal model of the Superbuck converter has been derived [18], indicating the transfer function between output (V_{out}) and control signal (d).

$$\begin{aligned}
 G_{vd}(s) &= \frac{\hat{V}_{out}}{\hat{d}} \\
 &= V_{in} \frac{(L_1 + L_2)C_1 s^2 - (DL_1 - D'L_2)\frac{D}{R}s + 1}{L_1 L_2 C_1 C_2 s^4 + \frac{L_1 L_2 C_1}{R} s^3 + [C_1(L_1 + L_2) + C_2(D^2 L_1 + D'^2 L_2)]s^2 + \frac{1}{R}(D^2 L_1 + D'^2 L_2)s + 1} \\
 &= V_{in} \frac{(L_1 + L_2)C_1 s^2 - (DL_1 - D'L_2)\frac{D}{R}s + 1}{h_4 s^4 + h_3 s^3 + h_2 s^2 + h_1 s + 1} \\
 h_4 &= L_1 L_2 C_1 C_2, \quad h_3 = \frac{L_1 L_2 C_1}{R}, \quad h_2 = C_1(L_1 + L_2) + C_2(D^2 L_1 + D'^2 L_2), \quad h_1 = \frac{1}{R}(D^2 L_1 + D'^2 L_2)
 \end{aligned} \tag{1}$$

In the frequency domain exist two vital system targets, the Amplitude Margin (AM) and Phase Margin (PM), which represent the distance to the critical steady state of the closed-loop system and signify the robustness of the whole system against the disturbance. The decrement of both AM and PM can forecast the potential fault and deterioration of the circuit system as an important indicator. As a result, it is significant to observe the performance of the recessive weakness in the frequency domain, including the cross frequency, amplitude margin, and phase margin.

The frequency performance of the Superbuck circuit with the single increment of L_1 , L_2 and both of L_1 & L_2 with 10% are tested as follow. Figure 3 shows the bode diagram within the recessive weakness of both inductance L_1 & L_2 (synchronously) and the single change of the inductance L_1 , L_2 in contrast to the normal situation. Table 2. show the system steady margin of the normal situation, single change of component, and recessive weakness. The AM and PM of a normal situation are 32.7 dB and 24.4°, while the margin of recessive weakness is drastically decreased in both AM and PM to 23.1 dB and 10.2° [19].

The results from the simulation in the frequency domain reveal the distinct deterioration of the whole Superbuck system with fault of recessive weakness. The normal operating situation is close to the single change of L_1 , L_2 with similar AM and PM in the frequency domain. However, the recessive weakness generated by both inductance L_1 & L_2 displays the reduced amplitude margin and phase margin dramatically, which means a weaker and worse system performance. So far, the recessive

weakness may bring serious and destructive damages to the system, without timely detection and protection approach.

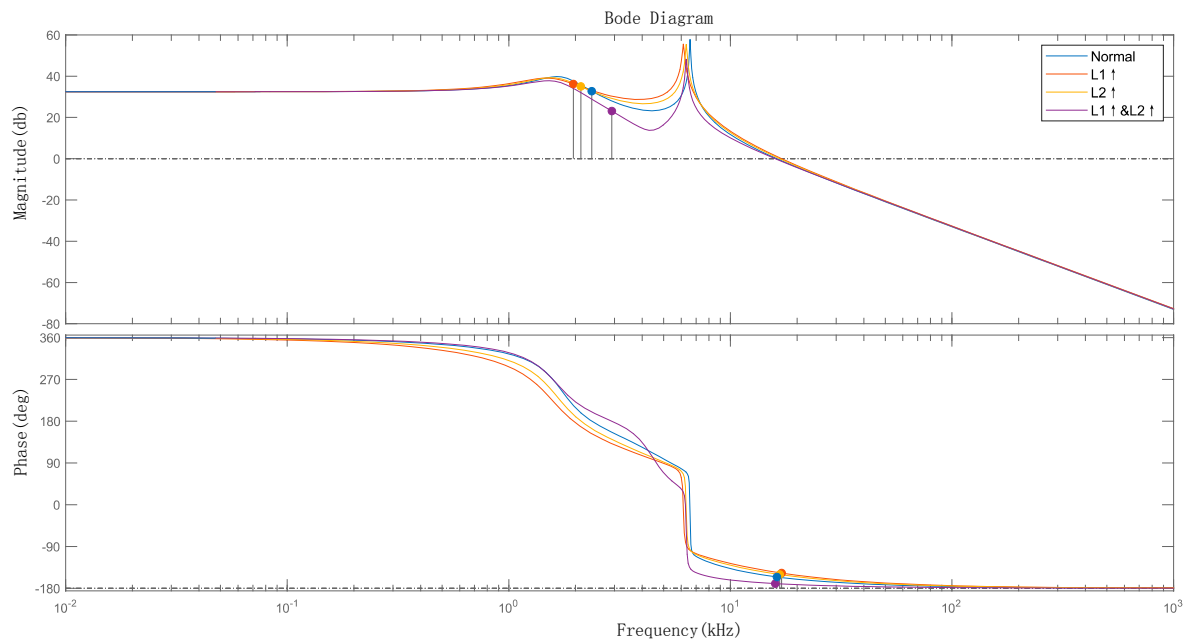


Figure 3. Bode diagram of Superbuck converter with recessive weakness.

Table 2. System Stability Margins.

	Cross Frequency (kHz)	Amplitude Margin (dB)	Phase Margin (deg)
Normal	16.2	32.7	29.4
$L_1 \uparrow$	17.0	36.2	32.8
$L_2 \uparrow$	16.7	35.0	29.7
$L_1 \uparrow$ & $L_2 \uparrow$	15.9	23.1	10.2

In conclusion, considering the performance and significance of recessive weakness in both time and frequency domain, a new method which focus on the recessive weakness is needed to solve the problem and ensure the normal operation of the power system. To solve against the phenomenon of the analogous character in a time domain and differential character in a frequency domain from recessive weakness, a new method to detect and classify this kind of soft fault in the circuit is proposed later in this paper.

3. Wavelet Packet Decomposition

3.1. Wavelet Theory

Wavelet transform is an effective and powerful approach to time-frequency analysis, which is developed from the foundation of overcoming the weakness of Fourier transform within a non-stationary signal [20]. Through wavelet transform, some invisible and hidden information in the time domain can be clearly revealed. Wavelet transform has been broadly applied in lots of fields, such as signal processing, image processing, pattern recognition and data compression. One of the most important characters of the wavelet transform is the great localization of features in both the time domain and frequency domain, providing the frequency information by the frequency base of the original signal [21]. The significance of the wavelet transform is through the shift of the mother wavelet function, and then under different scale a to proceed with the transvection with signal $x(t)$.

$$CWT(a, \tau) = \int_{-\infty}^{+\infty} \frac{1}{\sqrt{a}} x(t) \varphi\left(\frac{t - \tau}{a}\right) dt \quad (2)$$

where a is the scale factor and τ is the time shift. In continuous wavelet transform, a , b and τ are all continuous in the time domain.

$$DWT(m, n) = \frac{1}{\sqrt{a_0^m}} \int_R f(x) \varphi\left(\frac{x - nb_0 a_0^m}{a_0^m}\right) dx \quad (3)$$

where $\varphi_{m,n}(x) = \frac{1}{\sqrt{a_0^m}} \varphi\left(\frac{x - nb_0 a_0^m}{a_0^m}\right)$ $m, n \in Z$ is the wavelet basis, a_0, b_0 are constant and $a_0 > 0$.

3.2. Wavelet Packet Decomposition

The aim of WPD is to develop the representation forms of the analyzed signal $f(t)$ according to the scale and wavelet function [22]. The WPD deals with not only low frequency but also high frequency and contains possibly more information of the original sampled signal. The procedure of WPD is shown in Figure 4, where $x(n)$ is the sampled form of the original signal $f(t)$, $h_{ij}(n)$ $l_{ij}(n)$ represent the high frequency and low frequency decomposition coefficient in each level respectively, i is the decomposition level, j is the array of the decomposition results.

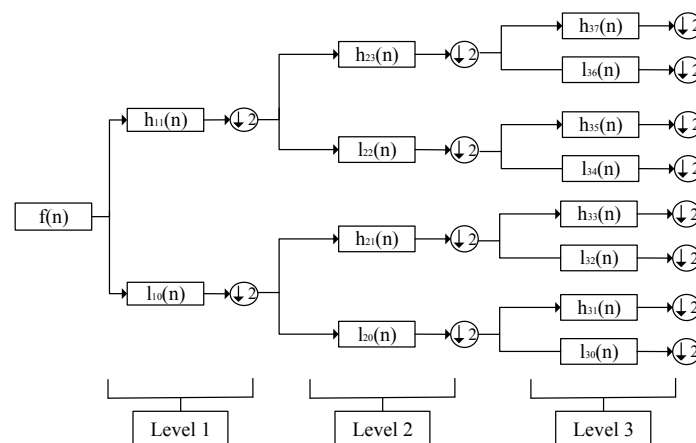


Figure 4. The process of three-level wavelet packet decomposition.

3.3. Decomposition Level

In theory, the higher the decomposition level, the more complete and accurate information is reserved without missing the original features [23]. However, with the increasing of the decomposition level, the computation time grows also significantly meanwhile. Thus, the option of a proper decomposition level is significant, which considers both the number of candidate features and computation time. Through the selected mother wavelet, a data-independent selection (DIS) method is proposed [24] to determine the wavelet decomposition level appropriately. The steps of the DIS approach is based as follows.

The specific wavelet composition level (n_{Ls}) to be assumed depends on the sampling frequency f_s of the measured original signal. For the sake of allowing the high level signals (concluding both approximation and details) to cover all the regions of frequencies along the localized sideband. The sideband components are generally identified as the harmonic components of the signal, that occur around the both sides of the fundamental frequency components.

The minimum number of the wavelet decomposition level that is necessary to obtain an approximation signal compared to the original signal therefore reveals that the upper limit of the associated frequency band remains under the signal frequency:

$$2^{-(n_{LS}+1)} f_s < f \quad (4)$$

From this, the decomposition level of the approximation signal should be as the integer n_{LS} , given by:

$$n_{LS} = \text{floor} \left| \left(\frac{\log(f_s/f)}{\log(2)} \right) \right| \quad (5)$$

where $\text{floor} \left| \right|$ means to take the integral part of the calculation result of the formula.

In the actual application situation, a further decomposition level of the original signal is advised and adopted, leading to the signal frequency band $[0, f]$, which can be possibly decomposed into more frequency bands. Ordinarily, two more extra wavelet decomposition level [24], $n_{LS} + 2$, would be adequate for the wavelet packet decomposition analysis. In this paper, we consider 9 as the proper decomposition level.

4. Feature Extraction

Without taking the detail and approximation coefficient of the wavelet packet decomposition results immediately as the input of the classifier, the feature extraction is necessary to improve the process of classification. Statistical methods, such as mean, standard deviation, rms, skewness and log-energy entropy are used as the feature extractors but show less robustness with noises [25]. Consequently, in this paper, we recommend taking the energy based method to feature extraction in virtue of Parseval's theorem.

4.1. Parseval's Theorem

When the recessive weakness occurs in a Superbuck converter, the energy space distribution of the output character alters accordingly, which indicates that the variation of output energy contains enough related character information. Since the selected mother wavelet and the scale function are mutually orthonormal, then the energy spectrum of each level of the WPD can be acquired, described by Parseval's theorem [26].

$$E_{\text{signal}} = \sum_{j=0}^{\infty} \sum_{k=-\infty}^{\infty} |c_j(k)|^2 + \sum_{j=0}^{\infty} \sum_{k=-\infty}^{\infty} |d_j(k)|^2 \quad (6)$$

$$E_{\text{signal}} = \sum_{j=0}^{J-1} E_{cj} + \sum_{j=0}^{J-1} E_{dj} \quad (7)$$

$$E_{cj} = \langle c_j(k), c_j(k) \rangle = \|c_j\|_2^2 \quad (8)$$

$$E_{dj} = \langle d_j(k), d_j(k) \rangle = \|d_j\|_2^2 \quad (9)$$

where J stands as the number of the WPD scale.

In aim to enhance the features, the difference between energy E_{fault} caused by recessive weakness and energy E_{normal} in a normal operating situation together derives the feature energy ΔE . The adopted feature vector can be mathematically represented as the following form:

$$f = \begin{bmatrix} f_1 \\ \vdots \\ f_i \\ \vdots \\ f_{\max} \end{bmatrix} = \begin{bmatrix} E_{\text{fault}.1} \\ \vdots \\ E_{\text{fault}.i} \\ \vdots \\ E_{\text{fault}.\max} \end{bmatrix} - \begin{bmatrix} E_{\text{normal}.1} \\ \vdots \\ E_{\text{normal}.i} \\ \vdots \\ E_{\text{normal}.max} \end{bmatrix} = \begin{bmatrix} \Delta E_1 \\ \vdots \\ \Delta E_i \\ \vdots \\ \Delta E_{\max} \end{bmatrix} \quad (10)$$

The more outstanding the difference between normal and fault energy is, the more related and useful information used for classification are included in the result of the wavelet packet decomposition [27].

4.2. Principal Component Analysis

Giving consideration to the vector space, calculating quantity and network repose time, the energy feature vector gained from the wavelet packet decomposition must be further dimension reduced. To reduce the feature dimension, PCA is generally applied to the extracted features [28].

PCA was for the first time proposed by Kirby in 1990, which projected the original sample space into the lower dimensional space to reduce the data dimension, remove the unnecessary attributes, eliminate redundant information so as to decrease the time of fault detection, and improve the detection efficiency. As a useful statistical process technique, PCA maintains the features with more information contribution, the remaining features can still reflect and reserve the large majority of the information from the original data [29].

For a feature vector set $F_{n \times p}$, consisting of p vectors with n elements, the orthogonal axes w_j are given by

$$Sw_j = \lambda_j w_j \quad (11)$$

where S is the covariance matrix of the vector set (T) and λ_j stands the eigenvalue related to the eigenvector (w_j) of the S .

Assuming the original vector sample contains n dimension eigenvectors $X_K = (x_1, x_2, x_3, \dots, x_n)^T$ in sum of N , the principal component method to the data analysis are as follows:

- (1) Calculate the mean of each dimension

$$\bar{x}_l = \frac{1}{N} \sum_{i=1}^N x_i \quad (12)$$

- (2) Obtain the covariance matrix from the mean of the data, as follows:

$$S = \frac{1}{N} \sum_{i=1}^N (x_i - \bar{x}_l)(x_i - \bar{x}_l)^T \quad (13)$$

where the dimension of Covariance S is $R \times R$.

- (3) Figure the eigenvalue $[\lambda_1, \lambda_2, \lambda_3, \dots, \lambda_R]$ of the covariance S , and the normalized eigenvector $[w_1, w_2, w_3, \dots, w_R]$ corresponding to the nonzero eigenvalue.

- (4) Sort the eigenvalues, the larger the eigenvalues are, implies the more prominent contribution the vector involved from the original signal.

- (5) Select the most principal component with sufficient contribution accumulation as the mapping matrix to transform the original feature vector into the new feature space.

$$Y = W^T X_k \quad (14)$$

The achieved energy feature vector from WPD is of high dimension data, which may influence the computing time and classification accuracy. To perform the more adequate input of classifier, the high dimension vector needs to be reduced. PCA can map the high dimension data to the low dimension feature space through linear transform based on the analysis of all features. After the dimension reduction, the most contributing feature vector will be reserved and remained. Therefore, the low dimension space has the ability to reflect the most important information from the original data.

In this paper, the original dimension of feature vector is 9, we take target dimension as 7 according to the simulation results.

4.3. Feature Extraction Results

Applying the WPD feature extraction method with 10db mother wavelet within Parseval's theory, the detailed energy distributions in different decomposition level of the output signal, including normal condition and recessive weakness are represented in Figure 5, respectively. The x -axis is the decomposition level while the y -axis the energy. The distinction between the normal situation and recessive weakness calculated through (10) is shown in Figure 6.

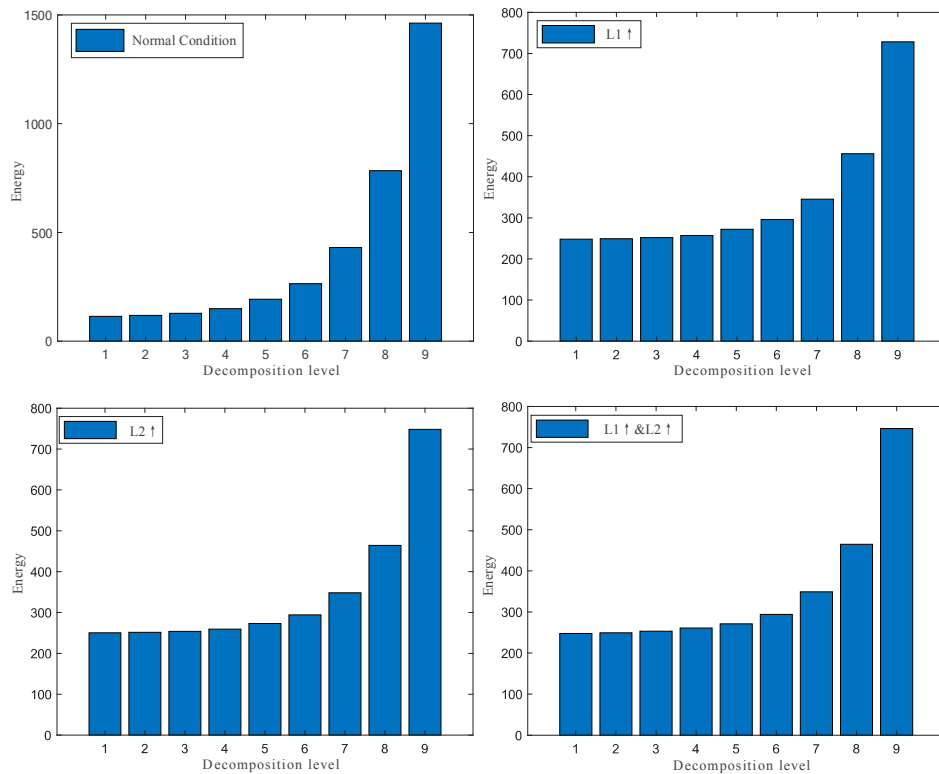


Figure 5. The result of wavelet packet decomposition (WPD) to the recessive weakness in the different level.

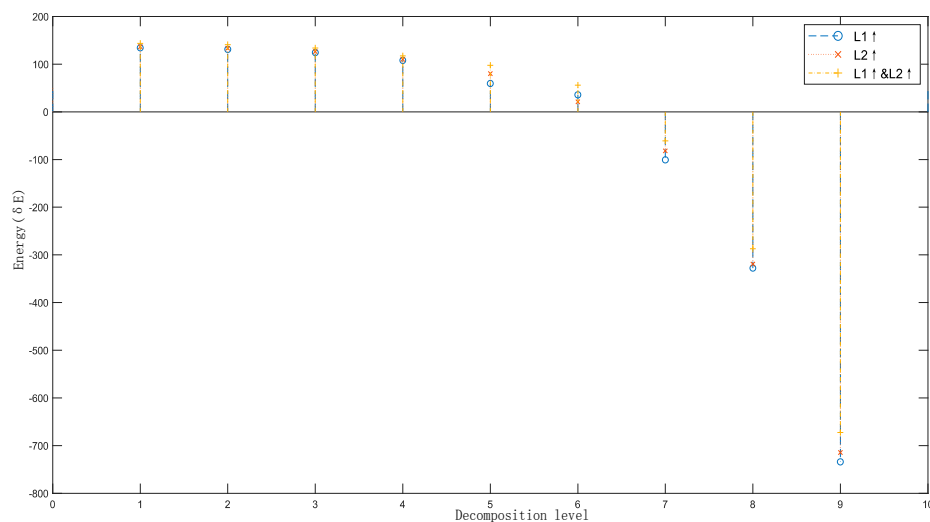


Figure 6. The distinction between normal condition and recessive weakness.

Through the above analysis, it can be concluded that the application of WPD and Parseval's theorem maintains the outstanding features of the invisible fault. In order to achieve less computing

time and memory space, PCA is an appropriate way to reduce dimensionality instead of using the results of WPD for the classification stage directly. The obtained data after the process of PCA are then utilized as the input vectors of PNN for pattern recognition, which is discussed in detail in the following part.

5. Probabilistic Neural Network

5.1. Probabilistic Neural Network

Probabilistic neural network (PNN) is a feed-forward artificial neural network (ANN) proposed by Specht D.F in 1990, which is based on the Bayes strategy of decision conducting and nonparametric estimators of conditional probability density functions [30]. The most significant advantage of PNN over other network models is its simple and instantaneous training process using all the samples without learning and its guarantee of asymptotical approaching the Bayes' optimal decision surface provided by the smooth and continuous class [31]. The structure of the PNN is demonstrated in Figure 7.

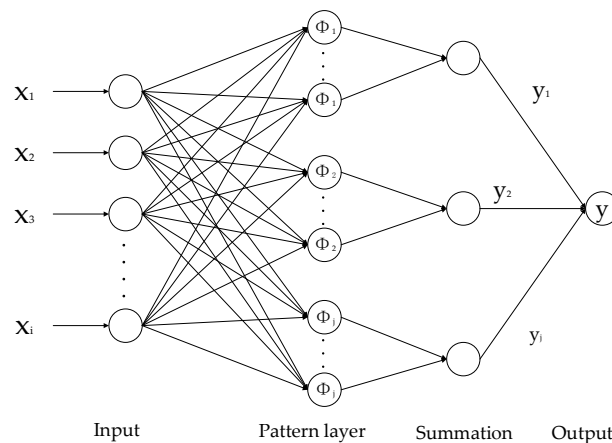


Figure 7. The structure of Probabilistic neural network.

The fault diagnosis method based on PNN uses the strong nonlinear classification ability of the model to map the fault sample space into the fault mode space, so as to form a diagnosis network system with strong fault tolerance and structure adaptive ability [6]. Compared with the BP network, the main advantages of PNN are:

- (1) Fast training, the training time is only slightly more than the interval of reading data.
- (2) No matter how complex the classification problem is, the optimal solution under Bayesian criterion can be guaranteed through enough training data.
- (3) Allowance of the increment and decrement of training data without long period of retraining time.

The classification process of PNN can be summarized as following steps:

- (1) Normalize the training samples and test samples.

$$x = \frac{x}{|x|} \quad (15)$$

$$X = \frac{X}{|X|} \quad (16)$$

x remains training data, X remains test data.

- (2) Send the normalized training samples x to the input layer directly.

(3) Calculate the distance of related elements between training samples and test samples.

$$E = \begin{pmatrix} \sqrt{\sum_{k=1}^n |X_{1k} - x_{1k}|^2} & \sqrt{\sum_{k=1}^n |X_{1k} - x_{2k}|^2} & \dots & \sqrt{\sum_{k=1}^n |X_{1k} - x_{mk}|^2} \\ \sqrt{\sum_{k=1}^n |X_{2k} - x_{1k}|^2} & \sqrt{\sum_{k=1}^n |X_{2k} - x_{2k}|^2} & \dots & \sqrt{\sum_{k=1}^n |X_{2k} - x_{mk}|^2} \\ \vdots & \vdots & \ddots & \vdots \\ \sqrt{\sum_{k=1}^n |X_{pk} - x_{1k}|^2} & \sqrt{\sum_{k=1}^n |X_{pk} - x_{2k}|^2} & \dots & \sqrt{\sum_{k=1}^n |X_{pk} - x_{mk}|^2} \end{pmatrix} = \begin{pmatrix} E_{11} & E_{12} & \dots & E_{1m} \\ E_{21} & E_{22} & \dots & E_{2m} \\ \vdots & \vdots & \ddots & \vdots \\ E_{p1} & E_{p2} & \dots & E_{pm} \end{pmatrix} \quad (17)$$

X_i is the training samples, $i = 1, 2, \dots, p$;

x_j is the test samples, $j = 1, 2, \dots, m$;

E_{ij} represent the Euclidean distance between X_i and x_j .

(4) Calculate the probability through Gaussian function.

$$p = \begin{pmatrix} p_{11} & p_{12} & \dots & p_{1m} \\ p_{21} & p_{22} & \dots & p_{2m} \\ \vdots & \vdots & \ddots & \vdots \\ p_{p1} & p_{p2} & \dots & p_{pm} \end{pmatrix} \quad (18)$$

$$p_{ij} = \exp\left(-\frac{E_{ij}}{2\sigma^2}\right) \quad (19)$$

(5) Adopt the competition function in the output layer according to the Bayesian discriminant and the maximum output of the summation layer is the fault kind x_j belongs to.

5.2. Structure of the Proposed Algorithm

The proposed fault detection and classification algorithm is based on the signature analysis of the sampled operating signals, performed by the WPD and PCA techniques to the feature extraction and dimensionality reduction of data while PNN is used for the fault classification [32]. The flowchart of the proposed algorithm is shown in Figure 8. In the step of data acquisition, the output voltage of the Superbuck converter is selected as the sampled signal for fault diagnostic. Then, the WPD is used to decompose every signal into a different level, including both low frequency and high frequency information. Parseval's theory is also utilized for the feature extraction of each sampled data. The extracted feature vectors are then run through the PCA to reduce the dimensionality of the vectors, which is used as the inputs of the PNN classification. The outputs of the neural network indicate the type of the recessive weakness (normal, single, couple, triple circuit components) that may occur in the Superbuck converter as the most likely recessive faults.

WPD in the proposed algorithm transfers the time domain information to the frequency domain. As demonstrated in Figures 2 and 3, the performance of recessive weakness express similarity in time and prominence in frequency. WPD through the wavelet transforms both high and low frequency information to contain possibly more information of the original sampled signal. As discussed, we take the db10 wavelet as the mother wavelet and nine as decomposition level properly. The coefficient of each decomposition level constructs the energy feature vector including both tendency and detail information. The utilizing of WPD is for the construction of a feature vector to the classifier. The results of WPD can clearly distinguish the kind of recessive weakness.

PCA in a proposed algorithm cannot only reduce the dimension of the feature vector but also lower the calculation amount. As demonstrated in Figure 6, the first several decomposition level results of WPD to different kinds of recessive weakness is approximate. Through PCA, the dimension of the feature vector can be reduced to seven instead of nine finally, which still reserves the most

prominent fault signal information. Less calculation time and more exact classification accuracy can be achieved by the application of PCA. Besides, PCA can also accelerate the convergence of the network and also perform the function in de-noising. Thus, PCA is more conducive to the fault detection and classification of recessive weakness.

The detection and classification method not only reduces the required data for the training of the network but also improves the speed of the calculation and operation. Besides, the purpose of the proposed method in this paper is to obtain an available and practical detector and classifier as a fault diagnosis, which can recognize and distinguish the causes of the recessive weakness before the proper mitigating actions can be taken. Moreover, the result of this method can be viewed as a forewarning towards the operation situation of the circuit system, accurately forecasting the trend of the converter in the future.

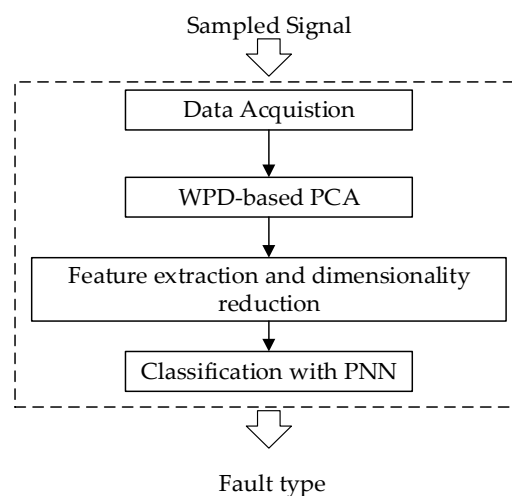


Figure 8. Flowchart of the proposed algorithm.

There also exists system uncertainty in the proposed algorithm. Some kinds of converters operate in DCM (Discontinuous Current Mode) in the condition of heavy load. Thus, the output voltage may be unsteady because of the switch in the operating mode [33]. The discontinuous voltage influences the uncertainty of the algorithm. Besides, the process of generating control command signals produce modeling uncertainties and other external disturbances [34]. There also present uncertainties in measurement and processes which may lead to false-alarm situations [35]. The parameter identification errors influence the data-driven fault detection design as well [36].

6. Experimental Analysis

The Supberbuck converter consists of four source components, L_1 , L_2 , C_1 , C_2 , which are utilized to verify the effectiveness of the proposed method in this paper. The efficiency and function of C_2 is just a wave filter in the circuit, therefore we design the verification experiment of the proposed algorithm regardless of C_2 . Thus, the verification experiment focuses on L_1 , L_2 and C_1 .

Meanwhile, the electrolytic capacitance is composed of cathode metal, oxide film, and electrolyte. The energy storage is based on the principle of electrostatic storage, the electrochemistry, and the structure of the electrode is in stability. The reason for the ageing problem consists in external stress, auto acceleration, and manufacturer factor and so on. According to the previous research, the capacitance becomes larger instead of smaller under the condition of high temperature and long-time use [37]. Therefore, the numerical value of C_1 usually becomes larger gradually with the ageing of the capacitance. Only the increment condition of C_1 is considered in this paper.

The inductor is generally constructed of a frame, winding, shielding cover, encapsulates material and others. The cause of the inductance variation includes the change of temperature, the damage of magnets and the rack of fusion. The operating frequency and different material also have great

impact on the inductor. With these complicated condition, the trend of inductance is unpredictable [38]. The inductance changing trend usually has the possibility of both wax and wane. With regard to the variation tendency of the inductance, both situations need to be considered within the verification experiments in this paper.

In sum, there exist in total 17 situations to test and verify the proposed algorithm, which conclude the single, double and triple changes of the components within L_1 , L_2 , C_1 . All the variation in both sides of L_1 , L_2 , C_1 are settled from 5% to 15% according to the normal distribution in the standardized test, which is described by Table 3.

Table 3. Classification Results.

	Situation	Training	Testing	Accuracy
F1	$C_1 \uparrow$	30	50	94%
F2	$L_1 \uparrow$	30	50	92%
F3	$L_1 \downarrow$	30	50	92%
F4	$L_2 \uparrow$	30	50	92%
F5	$L_2 \downarrow$	30	50	96%
F6	$C_1 \uparrow \& L_1 \uparrow$	30	50	92%
F7	$C_1 \uparrow \& L_1 \downarrow$	30	50	92%
F8	$C_1 \uparrow \& L_2 \uparrow$	30	50	90%
F9	$C_1 \uparrow \& L_2 \downarrow$	30	50	90%
F10	$L_1 \uparrow \& L_2 \uparrow$	30	50	92%
F11	$L_1 \uparrow \& L_2 \downarrow$	30	50	94%
F12	$L_1 \downarrow \& L_2 \uparrow$	30	50	88%
F13	$L_1 \downarrow \& L_2 \downarrow$	30	50	90%
F14	$C_1 \uparrow \& L_1 \uparrow \& L_2 \uparrow$	30	50	100%
F15	$C_1 \uparrow \& L_1 \uparrow \& L_2 \downarrow$	30	50	96%
F16	$C_1 \uparrow \& L_1 \downarrow \& L_2 \uparrow$	30	50	92%
F17	$C_1 \uparrow \& L_1 \downarrow \& L_2 \downarrow$	30	50	100%

The training and testing samples involve different kinds of recessive weakness (caused by two components simultaneously and three components simultaneously), normal situation, and the single change of the component. 30 samples are used for the training of each scenario with the proposed algorithm. 850 samples are utilized for testing, which cover the range of 17 fault kinds with 50 test samples.

The experiment results of the test samples are summarized in Table 3. The overall test classification accuracy achieves 93.05%, which shows the effectiveness of the proposed method to correctly classify the recessive weakness in the Superbuck converter.

It is clearly noted from Figure 9, the proposed method in this paper shows the great robustness to the different sorts of recessive weakness. The designed scheme has been proved and it has the generality for different recessive weakness and operating conditions.

Furthermore, the recessive weakness is beyond the normal tolerance range of the components and less than the total invalidation of system. Recessive weakness can represent the crucial transient process from normal operation to system failure. The meaning of detecting recessive weakness is to find out the abnormal operating situation before the complete invalidation of the circuits. The ordinary error range of inductance and capacitance is close to 5%. The changing range of recessive weakness in this paper is only 5–15%, which can still achieve high classification accuracy with 93.05%. With a larger changing range of components, the classification accuracy can be further improved. The purpose of this paper is to introduce the fault of recessive weakness and propose a useful detection method.

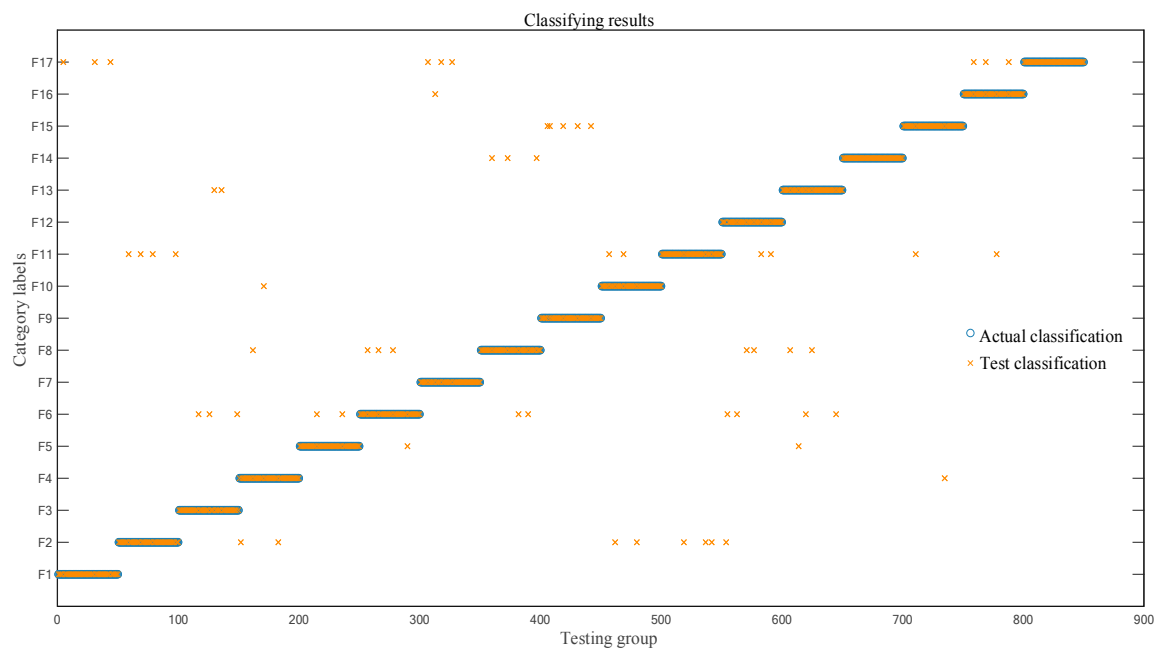


Figure 9. The results of the classification with proposed method.

7. Conclusions

This paper proposes a method that integrates the WPD technique combined with PCA and PNN for the fault detection and classification of recessive weakness in a Superbuck converter. The character of recessive weakness in a circuit is announced by simulation in both the time and frequency domains. The WPD provides an effective way to extract the character of the signal at different frequency bands. The proposed algorithm decreases the computational burden since the reduction of the input data is through PCA. The PNN affords an intelligent method and criterion to the feature comparison. The PNN is then adopted to classify the extracted features and detect the recessive weakness automatically, with a strong ability for generalization and training mechanisms. A related simulation has been performed to identify the capability of this method in fault detection and classification and the consequence shows that prospective accuracy can be achieved to distinguish recessive weakness. The extracted features have excellent robustness to the different recessive weakness, including different sums of the changed component. The proposed fault diagnosis method is simple, accurate, and its effectiveness has also been verified through experimental results. Refer to the purpose of this paper is to introduce the recessive weakness among soft faults, which is extremely difficult to detect and influence the performance of the circuit. This work will help to improve the application of the Superbuck converter and to put the emphasis on recessive weakness as an important diagnosis index.

Author Contributions: Conceptualization, C.W. and J.Y.; Data curation, C.W. and F.L.; Formal analysis, C.W. and F.L.; Funding acquisition, J.Y.; Investigation, L.W.; Methodology, C.W.; Project administration, L.W.; Resources, L.W., J.Y. and F.L.; Software, C.W.; Supervision, L.W., J.Y. and F.L.; Validation, C.W.; Writing—original draft, C.W.; Writing—review & editing, C.W. and J.Y.

Funding: This research was funded by Shanghai Science and Technology Innovation Action Plan under Grant No. 16DZ1205000.

Acknowledgments: The authors would like to acknowledge the support from the School of Ocean and Earth Science in Tongji university under the project “Research on the power system of large-scale scientific cabled seafloor observatory networks”. The authors also would hope to express sincere thankfulness to the editors and anonymous reviewers for their valuable opinions and contributions.

Conflicts of Interest: The authors declare no conflict of interest. The funders had no role in the design of the study; in the collection, analyses, or interpretation of data; in the writing of the manuscript, or in the decision to publish the results.

References

1. Karppanen, M.; Arminen, J.; Suntio, T.; Savela, K.; Simola, J. Dynamical Modeling and Characterization of Peak-Current-Controlled Superbuck Converter. *IEEE Trans. Power Electron.* **2008**, *23*, 1370–1380. [\[CrossRef\]](#)
2. Sun, K.; Wu, H.; Cai, Y.; Xing, Y. A Power Conditioning Stage Based on Analog-Circuit MPPT Control and a Superbuck Converter for Thermoelectric Generators in Spacecraft Power Systems. *J. Electron. Mater.* **2014**, *43*, 2287–2292. [\[CrossRef\]](#)
3. Wang, L.; Yue, J.; Su, Y.; Lu, F.; Sun, Q. A novel remaining useful life prediction approach for superbuck converter circuits based on modified grey wolf optimizer-support vector regression. *Energies* **2017**, *10*, 459. [\[CrossRef\]](#)
4. Chang, C.S.; Xu, Z.; Khambadkone, A. Enhancement and laboratory implementation of neural network detection of short circuit faults in DC transit system. *IEE Proc.-Electr. Power Appl.* **2003**, *150*, 344–350. [\[CrossRef\]](#)
5. Li, H.; Zhang, Y.X. An algorithm of soft fault diagnosis for analog circuit based on the optimized SVM by GA. In Proceedings of the 9th Annual International Conference on Electronic Measurement & Instruments, Beijing, China, 16–19 August 2009; pp. 4251–4255.
6. Zhao, G.; Zhou, L.; Yang, Y. Soft Fault Diagnosis in Analog Circuit Based on Fuzzy and Direction Vector. In Proceedings of the 11th Annual IEEE Circuits & Systems International Conference on Testing & Diagnosis, Chengdu, China, 28–29 April 2009; pp. 61–75.
7. Fang, J.; Li, W.; Li, H.; Xu, X. Online Inverter Fault Diagnosis of Buck-Converter BLDC Motor Combinations. *IEEE Trans. Power Electron.* **2015**, *30*, 2674–2688. [\[CrossRef\]](#)
8. Poon, J.; Konstantakopoulos, I.C.; Spanos, C.; Panda, S.K.; Sanders, S.R.; Jain, P. Model-Based Fault Detection and Identification for Switching Power Converters. *IEEE Trans. Power Electron.* **2016**, *32*, 1419–1430. [\[CrossRef\]](#)
9. Ekici, S.; Yildirim, S.; Poyraz, M. Energy and entropy-based feature extraction for locating fault on transmission lines by using neural network and wavelet packet decomposition. *Expert Syst. Appl.* **2008**, *34*, 2937–2944. [\[CrossRef\]](#)
10. Jolliffe, I. Principal Component Analysis. In *International Encyclopedia of Statistical Science*; Springer: Berlin/Heidelberg, Germany, 2011; pp. 1094–1096.
11. Wasserman, P.D. *Advanced Methods in Neural Computing*; John Wiley & Sons, Inc.: New York, NY, USA, 1993; pp. 116–118.
12. Yu, S.; Zhu, K.; Diao, F. A dynamic all parameters adaptive BP neural networks model and its application on oil reservoir prediction. *Appl. Math. Comput.* **2008**, *195*, 66–75. [\[CrossRef\]](#)
13. Zhi, Y.B.; Jie, H.; Ming, Y.W. Low input current ripple Battery Charging Regulator based on coupled-inductor. In Proceedings of the 22th Annual IEEE International Conference on Power System Technology, Hangzhou, China, 24–28 October 2010.
14. Leppäaho, J.; Suntio, T. Solar-generator-interfacing with a current-fed superbuck converter implemented by duality-transformation methods. In Proceedings of the 24th Annual IEEE International Power Electronics Conference, Sapporo, Japan, 21–24 June 2010; pp. 680–687.
15. Leppäaho, J.; Suntio, T. Dynamic characteristics of current-fed superbuck converter. *IEEE Trans. Power Electron.* **2011**, *26*, 200–209. [\[CrossRef\]](#)
16. Antonino-Daviu, J.; Riera-Guasp, M.; Roger-Folch, J.; Martinez-Gimenez, F.; Peris, A. Application and optimization of the discrete wavelet transform for the detection of broken rotor bars in induction machines. *Appl. Comput. Harmon. Anal.* **2006**, *21*, 268–279. [\[CrossRef\]](#)
17. Mittal, A. Automated Optimization of an Integrated Circuit Layout Using Cost Functions Associated with Circuit Performance Characteristics. U.S. Patent Application 12/288,268, 22 April 2010.
18. Jia, P.; Zheng, T.Q.; Yan, L. Parameter Design of Damping Networks for the Superbuck Converter. *IEEE Trans. Power Electron.* **2013**, *28*, 3845–3859. [\[CrossRef\]](#)
19. Doyle, J.C.; Francis, B.A.; Tannenbaum, A.R. *Feedback Control Theory*; Springer: Boston, MA, USA, 2009.
20. Li, W.; Monti, A.; Ponci, F. Fault Detection and Classification in Medium Voltage DC Shipboard Power Systems with Wavelets and Artificial Neural Networks. *IEEE Trans. Instrum. Meas.* **2014**, *63*, 2651–2665. [\[CrossRef\]](#)

21. Yusuff, A.A.; Fei, C.; Jimoh, A.; Munda, J.; Jimoh, A.-G.A.; Munda, J. Fault location in a series compensated transmission line based on wavelet packet decomposition and support vector regression. *Electr. Power Syst. Res.* **2011**, *81*, 1258–1265. [\[CrossRef\]](#)
22. Zhang, Z.; Wang, Y.; Wang, K. Fault diagnosis and prognosis using wavelet packet decomposition, Fourier transform and artificial neural network. *J. Intell. Manuf.* **2013**, *24*, 1213–1227. [\[CrossRef\]](#)
23. Wang, D.; Miao, D.; Xie, C. Best basis-based wavelet packet entropy feature extraction and hierarchical EEG classification for epileptic detection. *Expert Syst. Appl.* **2011**, *38*, 14314–14320. [\[CrossRef\]](#)
24. Erişti, H.; Uçar, A.; Demir, Y. Wavelet-based feature extraction and selection for classification of power system disturbances using support vector machines. *Electr. Power Syst. Res.* **2010**, *80*, 743–752. [\[CrossRef\]](#)
25. Caesarendra, W.; Tjahjowidodo, T. A review of feature extraction methods in vibration-based condition monitoring and its application for degradation trend estimation of low-speed slew bearing. *Machines* **2017**, *5*, 21. [\[CrossRef\]](#)
26. Liao, C.C.; Yang, H.T. Recognizing Noise-Influenced Power Quality Events with Integrated Feature Extraction and Neuro-Fuzzy Network. *IEEE Trans. Power Deliv.* **2009**, *24*, 2132–2141. [\[CrossRef\]](#)
27. Ning, J. *Wide-Area Monitoring and Recognition for Power System Disturbances Using Data Mining and Knowledge Discovery (Dmkd) Theory*; Tennessee Technological University: Cookeville, TN, USA, 2010.
28. Abe, S. Feature selection and extraction. In *Support Vector Machines for Pattern Classification*; Springer: London, UK, 2010; pp. 331–341.
29. Gertler, J. *Fault Detection and Diagnosis*; Springer: London, UK, 2013.
30. Ahmadlou, M.; Adeli, H. Enhanced probabilistic neural network with local decision circles: A robust classifier. *Integr. Comput.-Aided Eng.* **2010**, *17*, 197–210. [\[CrossRef\]](#)
31. Muniz, A.; Liu, H.; Lyons, K.; Pahwa, R.; Liu, W.; Nobre, F.; Nadal, J. Comparison among probabilistic neural network, support vector machine and logistic regression for evaluating the effect of subthalamic stimulation in Parkinson disease on ground reaction force during gait. *J. Biomech.* **2010**, *43*, 720–726. [\[CrossRef\]](#) [\[PubMed\]](#)
32. Evagorou, D.; Lewin, P.; Efthymiou, V.; Kyprianou, A.; Georghiou, G.; Stavrou, A.; Metaxas, A.; Georghiou, G. Feature extraction of partial discharge signals using the wavelet packet transform and classification with a probabilistic neural network. *IET Sci. Meas. Technol.* **2010**, *4*, 177–192. [\[CrossRef\]](#)
33. Shabestari, P.; Gharehpetian, G.; Riahy, G.; Mortazavian, S. Voltage controllers for DC-DC boost converters in discontinuous current mode. In Proceedings of the 4th Annual IEEE International Energy & Sustainability Conference, Farmingdale, NY, USA, 12–13 November 2015.
34. Ghanaatian, M.; Lotfifard, S. Control of Flywheel Energy Storage Systems in Presence of Uncertainties. *IEEE Trans. Sustain. Energy* **2018**, *10*, 36–45. [\[CrossRef\]](#)
35. Boem, F.; Rivero, S.; Ferrari-Trecate, G.; Parisini, T. Plug-and-Play Fault Detection and Isolation for Large-Scale Nonlinear Systems with Stochastic Uncertainties. *IEEE Trans. Autom. Control* **2019**, *64*, 4–19. [\[CrossRef\]](#)
36. Dong, J.; Verhaegen, M.; Gustafsson, F. Robust Fault Detection with Statistical Uncertainty in Identified Parameters. *IEEE Trans. Signal Process.* **2012**, *60*, 5064–5076. [\[CrossRef\]](#)
37. Gu, S.; Wei, L.; Zhang, Y.; Yao, Y. Prospects of Ageing Characteristic and Life Test Research on Supercapacitors. *Proc. CSEE* **2013**, *33*, 145–153.
38. Xu, S.W. *Failure Analysis and Detection of the Key Devices of Switching Power Supply*; University of Electronic Science and Technology of China: Chengdu, China, 2013.

